



Predicting global landslide spatiotemporal distribution: Integrating landslide susceptibility zoning techniques and real-time satellite rainfall estimates

Yang HONG¹ and Robert F. ADLER²

Abstract

Landslides triggered by rainfall can possibly be foreseen in real time by jointly using rainfall intensity-duration thresholds and information related to land surface susceptibility. However, no system exists at either a national or a global scale to monitor or detect rainfall conditions that may trigger landslides due to the lack of sufficient ground-based observing network in many parts of the world. Recent advances in satellite remote sensing technology and increasing availability of high-resolution geospatial products around the globe have provided an unprecedented opportunity for such a study. In this paper, a framework for developing a preliminary real-time prediction system to identify where rainfall-triggered landslides will occur is proposed by combining two necessary components: surface landslide susceptibility and a real-time space-based rainfall analysis system (<http://trmm.gsfc.nasa.gov>). First, a global landslide susceptibility map is derived from a combination of semi-static global surface characteristics (digital elevation topography, slope, soil types, soil texture, land cover classification, etc.) using a GIS weighted linear combination approach. Second, an adjusted empirical relationship between rainfall intensity-duration and landslide occurrence is used to assess landslide hazards at areas with high susceptibility. A major outcome of this work is the availability for the first time of a global assessment of landslide hazards, which is only possible because of the utilization of global satellite remote sensing products. This preliminary system can be updated continuously using the new satellite remote sensing products. This proposed system, if pursued through wide interdisciplinary efforts as recommended herein, bears the promise to grow many local landslide hazard analyses into a global decision-making support system for landslide disaster preparedness and mitigation activities across the world.

Key Words: Landslide, Natural disasters, Satellite remote sensing, Real-time precipitation analysis, Landslide susceptibility

1 Introduction

Landslides are one of the most widespread natural hazards on Earth. In the U.S. alone landslides occur in every state, causing an estimated \$2 billion in damage and 25–50 deaths each year (USGS, 2006). Annual average loss of life from landslide hazards in Japan is 170 (Sidle and Ochiai, 2006). The situation is much worse in developing countries and remote mountainous regions due to lack of financial resources and inadequate disaster management ability. Recently, a landslide, triggered by "La Nina" rains, buried an entire village on the Philippines Island of Leyte on Feb 17, 2006, with at least 1,800 reported deaths and only 3 houses left standing of the original 300. A precipitation analysis using multiple satellites (Huffman

¹ Dr., Research Scientist, NASA Goddard Space Flight Center, Laboratory for Atmospheres, code 613.1, Greenbelt, MD 20771; Asso. Prof., School of Civil Engineering and Environmental Sciences, University of Oklahoma, Norman, OK 73019, U. S. A. Corresponding author: Phone: 1-405-325-3644; Fax: 1-405-325-4217; E-mail: yanghong@ou.edu, yanghong@agnes.gsfc.nasa.gov

² Dr., Senior Research Scientist, Code 613.1, Laboratory for Atmospheres, NASA/Goddard Space Flight Center, Greenbelt, MD 20771 U. S. A., Phone: (301) 614-6290; Fax: (301) 286-1626

Note: The original manuscript of this paper was received in April 2007. The revised version was received in May 2008. Discussion open until Sept. 2009.

et al., 2007), including National Aeronautics and Space Administration (NASA)'s Tropical Rainfall Measuring Mission (TRMM), reported that 500 millimeters of heavy rainfall fell on that area in a 10-day period (Lagmay et al., 2006). The need to develop more effective spatial coverage of landslide susceptibility and real-time hazard monitoring for vulnerable countries and remote areas remains apparent and urgent (Sidle and Ochiai, 2006).

Landslides triggered by rainfall can possibly be predicted by modelling the relationship between rainfall intensity-duration and landslide occurrence (Keefer and Wilson, 1987). Currently no system exists at a global scale to identify rainfall conditions that may trigger landslides, largely due to lack of field-based observing networks in many parts of the world. In particular, developing countries usually lack expensive ground-based monitoring networks. Thus, for many countries around the world, remote sensing information may be the only possible source of rainfall data and land surface characteristics available for such study. Recent advances in satellite-based precipitation observation technology and increasing availability of high-resolution geospatial products at global scale are providing an unprecedented opportunity to develop a real-time prediction system for a global view of rainfall-triggered landslides.

In this paper, a framework is proposed to develop a real-time prediction system for rainfall-triggered landslides around the globe. Drawing on the heritage of a space-based global precipitation observation system and remotely sensed surface characteristics products, this study first derives a global susceptibility map from the geospatial datasets and then links this analysis to the dynamic trigger, real-time rainfall observations, to assess landslide hazards. The goal of this new system is to acquire a global view, rather than a site-specific view, of rainfall-triggered landslide disasters in a real-time fashion.

2 A framework for predicting rainfall-triggered landslides at near real-time manner

In this study, we are primarily concerned with shallow landslides that involve poorly consolidated soils or colluviums on steep hill slopes. Shallow landslides, sometimes referred to as debris flows, mudslides, mudflows, or debris avalanches, are rapidly moving flows of mixes of rocks and mud, which have the potential to kill people and destroy homes, roads, bridges, and other property. This study addresses those landslides caused primarily by prolonged, heavy rainfall on saturated hill slopes characterized by high permeability. Rainfall-triggered landslides may mobilize into fast-moving mudflows, which generally present a greater hazard to human life than slow-moving, deep-seated slides. Although most parts of the world have experienced major socioeconomic losses related to landslide activity (Sidle and Ochiai, 2006), currently no system exists at either a regional or a global scale to identify rainfall conditions that may trigger landslides.

Useful assessment of landslide hazards requires, at the minimum, an understanding of both 'where' and 'when' that landslides may occur. As Fig. 1 shows, landslides result from a combination of factors, which according to (Dai and Lee, 2002) can be broadly classified into two categories: (1) preparatory variables that make the land surface susceptible to failure without triggering it, such as slope, soil properties, elevation, aspect, land cover, and lithology; and (2) the triggering events that induce mass movement, such as heavy rainfall and glacier outburst. For rainfall-triggered landslides, at least two conditions must be met: the areas must be susceptible to failure under certain saturated conditions, and the rainfall intensity and duration must be sufficient to saturate the ground to a sufficient depth. Therefore, to diagnose the landslide occurrence, the proposed system must link two major components: landslide susceptibility (LS) information and real-time precipitation analysis, as shown in Fig. 1. The LS map empirically shows part of the "where" and the rain intensity-duration primarily determines the "when" information. In use, the "where" LS map is overlaid with real-time satellite-based rainfall "when" layer to detect landslide hazards as a function of time and location.

In this framework, the first-order control on the spatial distribution (the "where") of landslides is the topographic slope of the ground surface, elevation, soil types, soil texture, vegetation, and the land cover classification, while the first-order control on the temporal distribution (the "when") of shallow landslides is the space-time variation of rainfall, which changes the pore-pressure response in the soil or colluviums to infiltrating water (Iverson, 2000).

Component 1: the dynamic trigger — space-borne real-time rainfall estimation

The spatial distribution, duration, and intensity of precipitation play an important role in triggering landslides. A long history of development in the estimation of precipitation from space has culminated in

sophisticated satellite instruments and techniques to combine information from multiple satellites to produce long-term products useful for climate monitoring (Adler et al., 2003). A fine time resolution analysis, such as the Tropical Rainfall Measuring Mission (TRMM) Multi-satellite Precipitation Analysis (TMPA) (Huffman et al., 2006), is the key data set for the proposed landslide monitoring system in this study. The TMPA global rainfall map is produced by using TRMM to calibrate, or adjust, the estimates from other satellite sensors, and then combining all the estimates into the TMPA final analysis. The coverage of the TMPA depends on input from different sets of sensors. First, precipitation-related passive microwave data are collected by a variety of low-Earth-orbit satellites, including the TRMM Microwave Imager (TMI) on TRMM, Special Sensor Microwave/Imager on Defense Meteorological Satellite Program (DMSP) satellites, Advanced Microwave Scanning Radiometer for the Earth Observing System (AMSR-E) on Aqua, and the Advanced Microwave Sounding Unit B (AMSU-B) on the National Oceanic and Atmospheric Administration (NOAA) satellite series. The second major data source for the TMPA is the window-channel (–10.7 micron) infrared (IR) data that are being collected by the international constellation of geosynchronous-Earth-orbit satellites, which provide excellent time-space coverage (half-hourly 4x4-km equivalent lat./long. grids) after merged by the Climate Prediction Center of the National Weather Service/NOAA (Janowiak et al., 2001). The IR brightness temperatures are corrected for zenith-angle viewing effects and inter-satellite calibration differences.

The TMPA is a TRMM standard product at fine time and space scales and covers the latitude band 50°N-S for the period 1998 to the delayed present. A real-time version of the TMPA merged product was introduced in February 2002 and is available on the NASA TRMM web site (<http://trmm.gsfc.nasa.gov>). Early validation results indicate reasonable performance at monthly scales, while at finer scales the TMPA is successful at approximately reproducing the surface-observation-based histogram of instantaneous precipitation over land, as well as reasonably detecting large daily events (Huffman et al., 2007). It is anticipated that this type of product will be continued as part of the Global Precipitation Measurement (GPM) mission (<http://gpm.gsfc.nasa.gov>). GPM is envisioned as improving the quality and frequency of observations from the constellation of operational and dedicated research satellites in order to provide improved global precipitation monitoring for hydrology and water resources management. Figure 2a shows a recent example of an instantaneous TMPA rain rate map downloaded from its web site. Figure 2b shows climatological percentage of daily rainfall exceeding 2 inches per day over land from 8 years of TMPA rainfall data (1998–2005). The availability of this type of rainfall information quasi-globally provides an opportunity to derive empirical rainfall intensity-duration thresholds related to landslides and to examine antecedent precipitation accumulation continuously in time and space.

Component 2: Global landslide susceptibility map

Previous research (Soeters and van Western, 1996) has grouped methods for landslide susceptibility and hazard assessment into inventory, heuristic, statistical and deterministic approaches. Fabbri et al. (2003) and Coe et al. (2004) indicated that topography was the dominant control in determining location of landslide occurrence. The effect of slope on landslides was documented by Dai and Lee (2002) and Lee and Min (2001). They reported slope steepness has the most influence on shallow landslide likelihood, followed by soil texture and soil types that mantle the slope. Vegetation on the slope is critical because bare slopes are especially vulnerable to erosion and mass wasting, but slopes with lush, healthy vegetation are far more resistant (Larsen and Sanchez, 1998). In addition, land cover can be classified into five classes: (a) forested land; (b) shrub land; (c) grass land; (d) pasture and cropland; (e) developed land and road corridors (Larsen and Sanchez, 1998), which describe a continuum of increasing susceptibility (e.g., from zero to one) to landslides.

Since it is not feasible to collect past landslide inventory data at the global scale, an approach that considers a numerical rating scheme for the factors contributing to landslide occurrence and a weighted linear combination method is applied to derive a final global landslide susceptibility map. This approach considers the integration of remote sensing and GIS techniques, given that most current models of the hazard prediction and landslide zoning are GIS-based or with the support of GIS (Metternicht et al., 2005). First, a central database collects several geospatial datasets at global scale. Second, important terrain factors contributing to landslide occurrence are derived and re-scaled to the highest NASA SRTM DEM spatial resolution (30m). These contributing factors include slope, soil types, soil texture, elevation, land use classification, and drainage density. Third, corresponding thematic data layers are generated and stored in

GIS; and finally the global susceptibility map is computed by performing a weighted linear combination function. The best model obtained was the one with weight determination (0.3, 0.2, 0.2, 0.1, 0.1, and 0.1) for the six parameters (slope, type of soil, soil texture, elevation, MODIS land cover type, and drainage density), respectively. The consequent range in susceptibility values is normalized from zero to one. The larger the susceptibility value, numerically, the greater the potential to produce landslide. The consequent range in susceptibility values is normalized from zero to 100. The larger the susceptibility value, the greater the landslide potential at that location. The landslide susceptibility values are then classified into several landslide susceptibility categories (Sarkar and Kanungo, 2004). A judicious way for such classification is to search for abrupt changes in values (Davis, 1986). The category boundaries are drawn at significant changes in the histogram of the landslide susceptibility values. As a result, the global landslide susceptibility map is finally classified into several categories, ranging from negligible to hotspot (Fig. 3). The very high and high susceptibility categories account for 2.8% and 18.6% of land areas. Figure 3 demonstrates the hot spots of the high landslide potential regions: the Pacific Rim, the Alps, the Himalayas and South Asia, Rocky Mountains, Appalachian Mountains, and parts of the Middle East and Africa. India, China, Nepal, Japan, the USA, and Peru are shown to be landslide-prone countries. These results are compatible to those reported by Sidle and Ochiai (2006). For more detailed description of global landslide susceptibility map, please refer to Hong et al. (2007).

3 A preliminary prediction system for rainfall-triggered landslides

3.1 Linking real-time rainfall triggers with landslide susceptibility information

There is a direct relationship between rainfall levels and the occurrence of landslides (Finlay et al., 1997), which, in return, depends on the properties of the soil surface (Irigray et al., 2000). This study links the global LS map with the frequently updated satellite-based precipitation information to identify when areas with high landslide potential are receiving heavy rainfall.

3.2 Preliminary results

Landslide hazard assessment based on relationships with rainfall intensity-duration has been applied at both global (Caine, 1980) and regional scales (Canuti et al., 1985; Larsen and Simon, 1993; Godt, 2004). Empirical rainfall intensity-duration thresholds have been developed for Seattle (Godt, 2004), Puerto Rico (Larsen and Simon, 1993), and worldwide (Caine, 1980). Hong et al. (2006) developed a satellite-based rainfall intensity-duration threshold as shown in Fig. 4. Note the squares indicate the rainfall intensity-duration plots of landslide events that occurred within the TRMM observation period. The lower bound of rainfall intensity-duration threshold was approximately identified ($\text{Intensity} = 12.45 \text{ Duration}^{-0.42}$). When coupled with real-time rainfall data, such rainfall intensity-duration thresholds might provide the basis for early warning systems for shallow landslides (Liritano et al., 1998). A preliminary prediction system for real-time landslide hazard assessment based on the adjusted rainfall intensity-duration threshold has been developed from these concepts and a trial version of this operational system is displayed on the NASA TRMM website (http://trmm.gsfc.nasa.gov/publications_dir/potential_landslide.html). The locations receiving rainfall exceeding the intensity-duration thresholds are marked as a landslide hazard zone if the underlying susceptibility category is “high” or “very high” at that location. The locations and timing of predicted landslides can then be checked against first-hand accounts from the field or validated by later news reports. This preliminary global prediction system for rainfall-triggered landslides is initially evaluated by comparing with reported landslide occurrences within the 8-year TRMM operational time period. For example, one landslide case was predicted by this preliminary system on 13 Apr 2006, in Colombia. The rainfall accumulation for the previous 24 hours was 103mm over central Colombia and the landslide susceptibility map indicates susceptibility category high at this area, so the landslide hazard is color-coded as red on the web-based graphical interface. Later news reports indicated that at least 34 people were missing and four villages were destroyed in a landslide near the Pacific port city of Buenaventura in southwestern Colombia. Table 1 lists 25 landslide occurrences collected from worldwide news reports, the TRMM website, and other sources. The calculated probability of detection (POD) is 0.76, 19 successful detections out of total 25 occurrences (Table 1). Among the 6 failures, 3 cases are caused by short-term heavy rainfall, 2 cases are by heavy rainfall on snow or snow melting, and one case is due to monsoon rainfall in India. This also demonstrates that the current algorithm does not work well for landslides

triggered by very intense rainfall in a relatively short time period (i.e., less than 12 hours) or by processes involving rapid snow melting. Despite variations among the cases, the production of shallow landslides obviously requires intense rainfall, sustained for at least a brief period of time, in areas with susceptibility category of “high” or above.

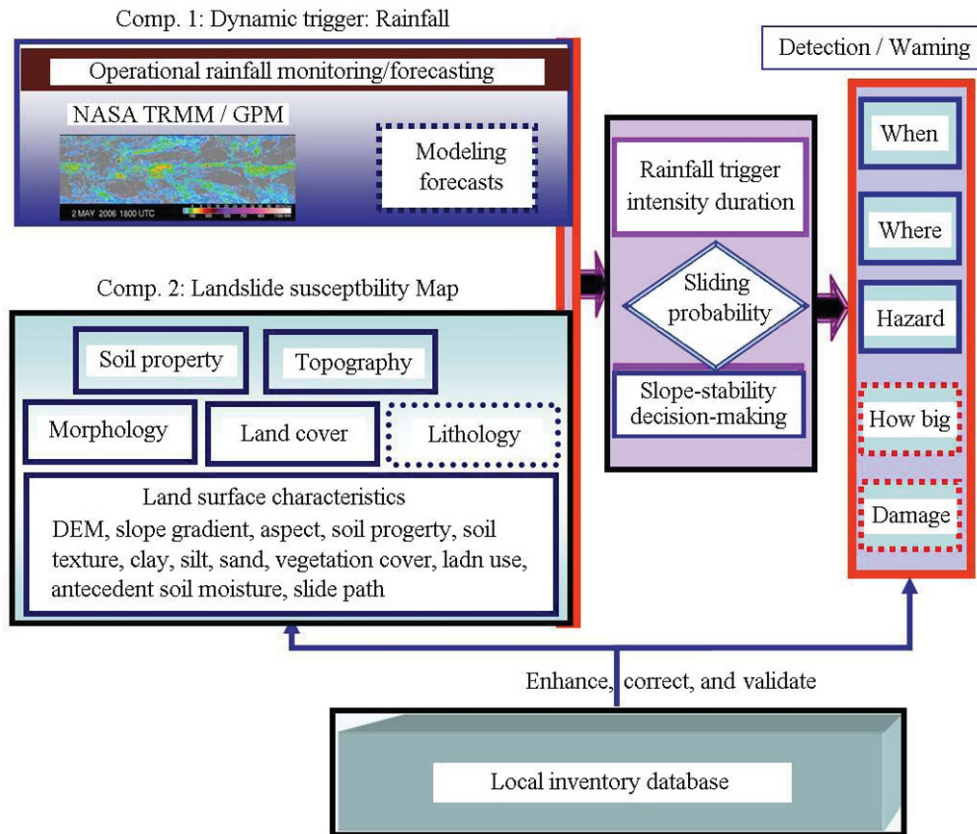


Fig. 1 The conceptual framework of real-time identifying/warning system for rainfall-triggered landslides at global scale. Note that dash-line boxes are important components but not covered in this study

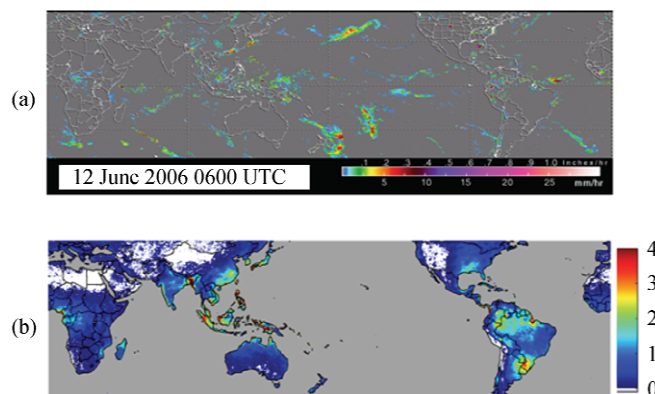


Fig. 2 NASA TRMM-based multi-satellite precipitation products: (a) real-time precipitation observations and (b) climatologic percentage of daily rainfall exceeding 2 inches

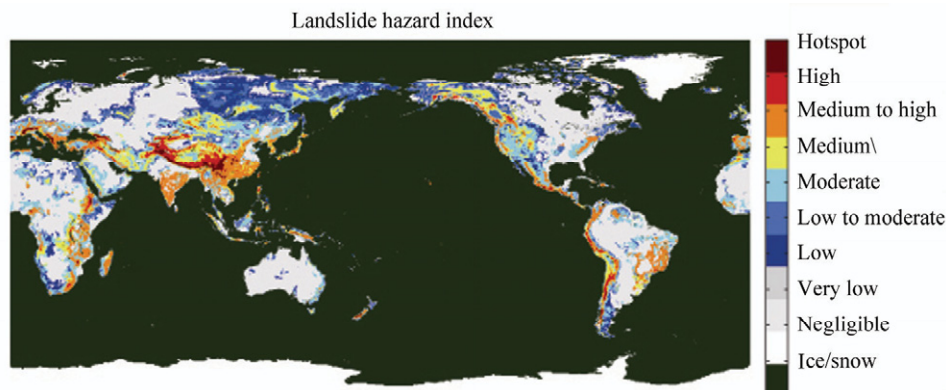


Fig. 3 Global landslide susceptibility map derived from surface multi-geospatial data

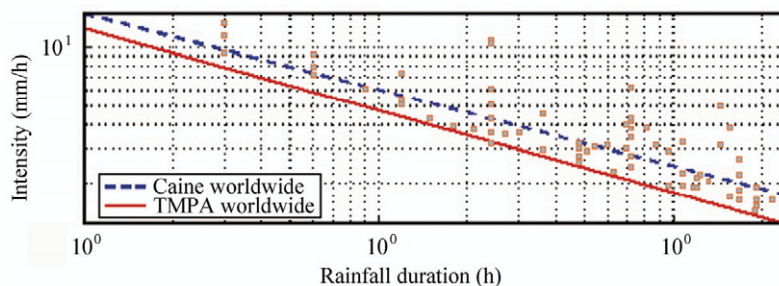


Fig. 4 Empirical rainfall intensity-duration threshold triggering landslides ($\text{Intensity} = 12.45 \text{Duration}^{-0.42}$) for landslides (squares) that occurred in the TRMM operation period (1998-2006). Note that dash line is Caine 1980

4 Summary and discussion

The primary criteria that influence shallow landslides are precipitation intensity, slope, soil type, elevation, vegetation, and land cover type. Drawing on recent advances in remote sensing technology and the abundance of global geospatial products, this paper proposed a conceptual framework for a real-time prediction system (Fig. 1) for rainfall-triggered landslides across the globe. This system combines the NASA TMPA precipitation information (Fig. 2; <http://trmm.gsfc.nasa.gov>) and land surface characteristics to assess landslides. First, a prototype of a global landslide susceptibility map (Fig. 3) is produced using high-spatial scale DEM, slope, soil type information downscaled from the Digital Soil Map of the World (sand, loam, silt, clay, etc.), soil texture, and MODIS land cover classification. Second, this map is overlaid with satellite-based observations of rainfall intensity-duration (Fig. 4), to identify the location and time of landslide hazards when areas with significant landslide susceptibility are receiving heavy rainfall. This preliminary landslide detection system shows promising effectiveness by comparing to recent landslide events that occurred during the TRMM operational period (Table 1). A major outcome of this work is the availability of a global prospective on rainfall-triggered landslide disasters, only possible because of the utilization of global satellite products. This type of real-time prediction system for disasters could provide policy planners with overview information to assess the spatial distribution of potential landslides. However, ultimate decisions regarding site-specific landslide susceptibility will continue to be made only after a site inspection.

A global evaluation of this system is underway through comparison with various field databases, web sites and news reports of landslide disasters. The need for retrospective validation and improvement of this preliminary system requires continued collection of global landslide data. The prototype of this system can be enhanced by providing improved satellite remote sensing products and by updating the geospatial database as more relevant information becomes available. Specifically, the land cover data should be routinely updated because they are subject to change by human activity. Several future activities are under consideration:

Table 1 Evaluation of the preliminary system by retrospectively comparing with reported worldwide landslides within last 8-year TRMM operational period (Note: mm = millimeters.)

Time	Country (State/Province)	Identified (Yes/No)	Causes/types	Major losses and damage
Aug. 22, 2006	Ban Thahan Village in Phang Nga, Thailand	No	Heavy rainfall/flash flood	Blocking the roads
Aug. 20, 2006	Holiday village of Gulval in Cornwall, UK	Yes	Heavy shower,	Unknown
Aug. 20, 2006	Surat Thani, Thailand	Yes	Heavy rainfall and flash flood	600 residents evacuated
Aug. 19, 2006	Song Bang town of northern mountainous Cao Bang province, Vietnam	Yes	Caused by prolonged heavy Rains	10 killed
Jul. 31, 2006	Roer Gulch east of Telluride, CO, USA	No	Heavy rainfall/flash flood	Unknown
Jul. 9	South Korea	Yes	Typhoon Ewinari, >300mm	Widespread mudslide
Jun. 28, 2006	Albany, upstate of NY	Yes	Heavy rainfall, 400mm/5 Days	2 killed
Jun. 25, 2006	Villages of Chamba District, Shimla, India	No	Strom, flash flood	Six houses swept away
Jun. 20, 2006	Sinjai in South Island of Sulawesi, Indonesian	Yes	Heavy rainfall >250mm	>200 deaths
May 17, 2006	The Schweitzer Mountain Ski resort, Sandpoint, Idaho	No	Rain on snow and snowmelt, rocks, mudslide, and debris flows	Condo buildings damaged
Apr. 13, 2006	Buenaventura, Colombia	Yes	Rainstorm, 103.04mm/day	>34 death
Jan. 04, 2006	Jakarta, Indonesia	Yes	Monsoon rains, 250mm/3day	>200 buried
Oct. 8, 2005	Solola, Guatemala	Yes	Hurricane Stan, 300mm/3day	>1,800 death
Sep. 5, 2005	Yuexi County, Anhui, China	Yes	Rain storm, 450mm/6day	210,000 people affected; 10,000 houses flattened
Aug. 5, 2005	Guwahati, India	No	Monsoon Rain, 310mm/3day	5 killed
Jan. 10, 2005	La Conchita, CA	Yes	Heavy rain season, 390mm/14day	12 death
Oct., 2004	Miyagawa area, Mie prefecture, Japan	Yes	Heavy and intense rainfall; Numerous landslides and debris flow	17 deaths, 9 injuries; 87 homes damaged/; extensive forest damage
Jul. 20, 2003	Minamata and Hishikari, southern Kyushu, Japan	Yes	Heavy and intense rainfall; Debris avalanches and debris flows	25 deaths; 7 homes destroyed; roads, power and hot spring lines damaged
May 2003	Ratnapura and Hambantota Districts, Sri Lanka	Yes	Continual heavy rains; Many landslides and debris flows	>260 deaths; > 24,000 homes/schools destroyed; 180,000 families homeless
May 11, 2003	Southwest Guizhou Province, China	Yes	Heavy rainfall and road construction; road-related landslides	35 road workers killed and 2 buildings and road destroyed
Apr. 20, 2003	Kara Taryk, Kyrgyzstan	No	Rain-on-snow; large landslides in Soviet-era uranium mining area	38 deaths; 13 homes destroyed; potential pollution of a river
Dec. 14-16, 1999	North coast of Venezuela near Caracas	Yes	Nearly, 1,000mm/3 days; Widespread shallow landslides and debris flows along a 40-km coastal strip	About 30,000 deaths; 8,700 residences infrastructure destroyed; extreme damage
Oct. 30, 1998	Casita Volcano, Nicaragua	Yes	Hurricane Mitch, 720mm/6day	>2,000 death
Aug. 26-31, 1998	Nishigo, Shirakawa, and Nasu, Japan	Yes	5 days of heavy rainfall; >1,000 landslides	9 deaths; many homes/buildings destroyed
Aug. 17, 1998	Malpa, Northern India	Yes	4 days of heavy rainfall; Large rockfall/debris avalanche	207 deaths; 5.2 million rupees direct cost and 0.5 million rupees indirect cost

- 1) More information, such as geologic factors, could be incorporated into this global landslide susceptibility map when they become available globally;
- 2) Finer resolution DEM data such as 6.1 x 6.1m LIDAR-based data can also improve the landslide susceptibility mapping, even if only available over small areas;
- 3) Soil moisture conditions observed from NASA Aqua satellite with the Advanced Microwave Scanning Radiometer-EOS (AMSR-E) instrument or an antecedent precipitation index accumulated from TRMM will be examined for usefulness in this preliminary landslide detection/warning system; and
- 4) The empirical rainfall intensity-duration threshold triggering landslides may be regionalized using mean climatic variables (e.g. mean annual rainfall).

Given the fact that landslides usually occur after a period of heavy rainfall, a real-time landslide prediction system can be readily transformed into an early warning system by making use of the time lag between rainfall peak and slope failure. Therefore, success of this prototype system bears promise as an early warning system for global landslide disaster preparedness and hazard management. Additionally, it is possible that the warning lead-time of global landslide forecasts can be extended by using rainfall forecasts (1-10 days) from operational numerical weather forecast models. This real-time prediction system bears the promise to extend current local landslide hazard analyses into a global decision-making support system for landslide disaster preparedness and mitigation activities across the world.

Acknowledgements

This research is carried out with support from NASA's Applied Sciences program under Steven Ambrose of NASA Headquarters and with support from University of Oklahoma.

References

- Adler R. F., Huffman G. J., Chang A., Ferraro R., Xie P., Janowiak J., Rudolf B., Schneider U., Curtis S., Bolvin D., Gruber A., Susskind J., and Arkin P. 2003, The version 2 Global Precipitation Climatology Project (GPCP) monthly precipitation analysis (1979–present). *Journal Hydrometeor*, Vol. 4, No. 6, pp. 1147–1167.
- Caine N. 1980, The rainfall intensity-duration control of shallow landslides and debris flows: *Geografiska Annaler*, v. 62A, pp. 23–27.
- Canuti P., Focardi P., and Garzonio C. A. 1985, Correlation between rainfall and landslide. *Bull. Int. Assoc. Eng. Geol.*, 32, pp. 49–54.
- Coe J. A., Godt J. W., Baum R. L., Bucknam R. C., and Michael J. A. 2004, Landslide susceptibility from topography in Guatemala, in: Lacerda and others (eds.), *Landslides: Evaluation and Stabilization*: London, Taylor and Francis Group, pp. 69–78.
- Dai F. C. and Lee C. F. 2002, Landslide characteristics and slope instability modeling using GIS. *Lantau Island, Hong Kong, Geomorphology* 42, pp. 213–238.
- Davis J. C. 1986, *Statistics and Data Analysis in Geology*, John Wiley & Sons, New York, N. Y., 646p.
- Fabbri A. G., Chung C. F., Cendrero A., and Remondo J. 2003, Is prediction of future landslides possible with GIS. *Journal of Natural Hazards* 30, pp. 487–499.
- Finlay P. J., Fell R., and Maguire P. K. 1997, The relationship between the probability of landslide occurrence and rainfall. *Canadian Geotechnical Journal* 34, pp. 811–824.
- Godt, J. 2004, *Observed and Modeled conditions for shallow landslide in the Seattle, Washington area*. Ph.D dissertation, University of Colorado, Boulder, CO.
- Hong, Y., Adler R. F., and Huffman G. 2006, Evaluation of the Potential of NASA Multi-satellite Precipitation Analysis in Global Landslide Hazard Assessment, *Geophysical Research Letter*, 33, L22402, doi:10.1029/2006GL028010.
- Hong, Y., Adler R. F., Huffman G., and Negri A. 2007, Use of satellite remote sensing data in mapping of global shallow landslides susceptibility. *Journal of Natural Hazards*, Vol. 43, No. 2, DOI: 10.1007/s11069-006-9104-z.
- Huffman G. J., Adler R. F., Bolvin D. T., Gu G., Nelkin E. J., Bowman K. P., Hong Y., Stocker E. F., and Wolff D. B. 2007, The TRMM Multi-satellite Precipitation Analysis: Quasi-Global, Multi-Year, Combined-Sensor Precipitation Estimates at Fine Scale. *Journal Hydrometeor*, Vol. 8, No. 1, pp. 38–55.
- Iverson, R. M. 2000, Landslide triggering by rain infiltration. *Water Resources Research*, Vol. 36, pp. 1897–1910.
- Janowiak J. E., Joyce R. J., and Yarosh Y. 2001, A Real-Time Global Half-Hourly Pixel-Resolution IR Dataset and Its Applications. *Bull. Amer. Meteor. Soc.*, 82, pp. 205–217.
- Keefer D. K. and Wilson R. C. 1987, Real-time landslide warning during heavy rainfall. *Science*, Vol. 238, No. 13, pp. 921–925.
- Lagmay A. M. A., Ong J. B. T., Fernandez D. F. D., Lapus M. R., Rodolfo R. S., Tengonciang A. M. P., Soria J. L. A., Baliatan E. G., Quimba Z. L., Uichanco C. L., Paguican E. M. R., Remedio A. R. C., Lorenzo G. R. H., Valdivia W.,

- and Avila F. B. 2006, Scientists Investigate Recent Philippine Landslide, EOS transaction, American Geophysical Union, Vol. 87, No. 12.
- Larsen, M. C. and Torres Sanchez A. J. 1998, The frequency and distribution of recent landslides in three montane tropical regions of Puerto Rico. *Geomorphology*, Vol. 24, pp. 309–331
- Larsen M. C. and Simon A. 1993, A rainfall intensity-duration threshold for landslides in a humid-tropical environment. *Puerto Rico: Geografiska Annaler*, Vol. 75A, pp. 13–23.
- Lee S. and Min K. 2001, Statistical analysis of landslide susceptibility at Yongin. Korea, *Environ Geol* 40:1095–1113.
- Liritano G., Sirangelo B., and Versace P. 1998, Real-time estimation of hazard for landslides triggered by rainfall. *Environmental Geology*; 35/2-3; pp. 175–183, Germany, Berlin: Springer-Verlag.
- Metternicht G., Lorenz H., and Radu G. 2005, Remote Sensing of Landslides: An analysis of the potential contribution to geo-spatial systems for hazard assessment in mountainous environments, *Remote Sensing of Environment* 98, pp. 284–303.
- Sarkar S. and Kanungo D. P. 2004, An integrated approach for landslide susceptibility mapping using remote sensing and GIS, *Photogrammetric Engineering & Remote Sensing*, Vol. 70, No. 5, May 2004, pp.617–625.
- Sidle R. C. and Ochiai H. 2006, *Landslide Processes, Prediction, and Land use*, Washington DC, American Geophysical Union, pp. 1–312.
- Soeters R. and van Westen C. 1996, Slope instability, recognition, analysis and zonation. In A. Turner, & R. Schuster (Eds.), *Landslides: Investigation and mitigation*. Special Report, Vol. 247, pp. 129–177, Washington DC Transportation Research Board, National Research Council, National Academy Press.
- USGS (United States Geological Survey) report. 2006, <http://landslides.usgs.gov/>